Developments in the Built Environment 20 (2024) 100576

Contents lists available at ScienceDirect

Developments in the Built Environment

journal homepage: www.sciencedirect.com/journal/developments-in-the-built-environment

Development of latex / silica aerogel composites for thermal insulation applications

Samuel Pantaleo *, Florent Gauvin, Katrin Schollbach, H.J.H. Brouwers

DEPARTMENT OF THE BUILT ENVIRONMENT, VERTIGO, Eindhoven University of Technology, PO BOX 513, 5600 MB, EINDHOVEN, the Netherlands

ARTICLE INFO

Keywords:
Innovative building materials
Energy efficiency
Building performance
Silica-aerogel
Thermal conductivity

ABSTRACT

Silica aerogel stands out as an exceptional thermal insulation material and is a great candidate for modern and energy-efficient buildings. However, silica aerogel also faces many challenges, mainly due to its expensive, unsustainable and difficult synthesis process, but also its poor structural properties. Consequently, the main research focus for silica aerogel is to mitigate its brittleness in order to pave the way for broader applications, especially in the building field. Therefore, this study focuses on the development of composite materials aiming at solving the abovementioned drawbacks of silica aerogel, by using environmentally friendly latexes and reinforcement that are easy to process. Results show the positive effect of this reinforcement, even at a small amount (5% volume), on the composite's properties, with thermal conductivity at least equivalent, or better, to either in development or already established insulation materials in the market.

1. Introduction

Nowadays, the building sector, including residential and commercial (non residential) building, is responsible for 36% of the total energy consumption and 37% of the global CO_2 emissions (a). These figures vary between countries depending on their economic development (Berardi, 2017). However, there is a shared commitment to reducing energy consumption and CO_2 emissions. To achieve this goal, governments are planning to implement new regulations and laws, which may be specific to certain sectors. Some regulations have already been put in place: For example, the Netherlands has decided to eliminate gas usage for newly built homes by 2050, thereby prohibiting their connection to the gas network. Other examples include research and development of green hydrogen as fuel and the use of biomass in various applications, such as building materials, raw components for industry, or energy sources (b). Similar policies can be observed worldwide ("Rénovation énergétique), (A. [D-N.-14] Rep. Ocasio-Cortez, 2019), encouraging refurbishment of houses and blocking renting if requirements are not fulfilled. Despite these efforts, the latest EU report (Jensen, 2020) indicates that the current pace of GHG reduction is insufficient to meet the target values for 2050, and therefore, further actions are required.

Based on the literature, a significant amount of global energy consumption and GHG emissions are related to housing purposes (a), (Lamb et al., 2021). Indoor temperature in homes or offices has a significant impact on humor, productivity, health, or perception of air quality (Zhang et al., 2011), (Chun et al., 2008). Poor thermal insulation causes heat loss, leading to increased energy consumption to maintain the same temperature, making it challenging to meet regulations with current materials. Thermal insulation techniques and materials have evolved since humans builts houses, from rock to biobased material to human-made materials. The main goals were every time to find more efficient material, but the space taken by the insulation material is nowadays a matter of importance aswell (Bozsaky, 2010). Table 1 shows a list of different conventional insulations with some specific values.

Therefore, to reach thermal conductivity values that may help fulfill the objectives, insulating materials with enhanced properties, previously unused, are now considered. Among them, aerogels (Gauvin et al., 2022), (Berger et al., 2020) catch the attention of the scientific community. They are lightweight (>99% air) which result in an increased amount of small pores, with a diameter smaller than the mean free path, making the Knudsen effect possible (Jelle et al., 2019). Aerogel can be organic or inorganic, and the most efficient, silica-based aerogels, can reach extremely low thermal conductivity, with values reported around 0.015 W m^{-1} K^{-1}, based on measurement techniques and conditions (Table 2). Concurrently, they also tend to be the most expensive option, because their synthesis, especially for large industrial quantities, still requires very specific conditions (Khudeev et al., 2024), (Gurav et al., 2010a) such as high pressure and temperature with a lot of energy

* Corresponding author.
E-mail address: s.m.pantaleo@tue.nl (S. Pantaleo).

https://doi.org/10.1016/j.dibe.2024.100576
Received 11 September 2024; Received in revised form 14 November 2024; Accepted 15 November 2024
Available online 20 November 2024

Table 1
Examples of material for thermal insulation.

Scientific articles				
Type of insulation	λ (W m^{-1} K^{-1})	**Process**	**Embodied energy (MJ)**	**Reference**
Mineral wool	0.030–0.046	Fiber spinning	37	(Abu-Jdayil et al., 2019), (Grazieschi et al., 2021)
EPS	0.030	Extrusion and CO_2 saturation	147	(Grazieschi et al., 2021), (Doroudiani and Kortschot, 2003), (Papadopoulos, 2005)
XPS	0.035	Extrusion and CO_2 saturation	144	(Grazieschi et al., 2021), (Doroudiani and Kortschot, 2003), (Papadopoulos, 2005)
Bio-based composites	0.045–0.060	Molding	6,8	(Koh et al., 2022), (Volk et al., 2024)
Mycelium composite	0.050–0.060	Mixing and molding	5,3	(Volk et al., 2024), (Gauvin et al., 2022)
Wood-wool cement board	0.060–0.075	Mixing with white cement	20	(Berger et al., 2020), (Hammond and Jones, 2008)

Commercially available product				
Name	**Declared λ (W m^{-1} K^{-1})**	**Material**	**Supplier**	**Reference**
SLS 20	0.035	Mineral granules	optiDämm	("Core insulation materials)
GUTEX Thermoflex ®	0.036	Wood fiber based	GUTEX	("GUTEX)
Slentite ®	0.017		BASF	("SLENTITE®." Accessed)
Gramittherm®	0.041	Grass board	Gramitherm Europe SA	("Produit)

required, explaining their high cost. However, research is being conducted to reduce production costs, explore new sources, and make the process more environmentally friendly (Chen et al., 2020), (Borzova et al., 2024), (Mermer and Piskin, 2018). Silica aerogels are suitable for different applications, because they can take different form, such as (nano)powder (drug deliveries (Soghra Jahed et al.), fiber coating (Soghra Jahed et al), thin films (Lin et al., 2023)), granulates (cement filling (Berardi and Nosrati, 2018), window glazing (Bin Rashid et al., 2023)) or monolithic (Bin Rashid et al., 2023). Despite their higher costs compared to more conventional thermal insulators (16–34 times more expensive than EPS (Li et al., 2023)), the exceptional properties of silica aerogels make them the most viable option when the primary concern is thermal conductivity. This is reflected in the increasing number of scientific papers on the subject over the past decade, particularly in the case of aerogels (Chruś et al., 2015).

While thermal conductivity is the key parameter for thermal insulation, additional characteristics such as moisture absorption, service life, strength, and fire resistance also need to be considered (see Fig. 1). In addition, the application of the material has to be considered. When the need is to minimize the impact on the current installation in a renovation, filling wall cavities is an excellent solution. Looking at wall cavities problematics (Fig. 2), silica aerogel granules (size $4 > x > 0.1$ mm) are the best option for this process compared to nano-powder, mainly looking at the thermal conductivity values and the feasibility of a wall cavity filling. However, silica aerogel cannot be used alone in the cavities due to its very low density, therefore a composite is required to ensure that the insulation remains in place for as long as possible.

Table 2
Comparison of aerogels and aerogel-based composites.

Type of insulation	λ (W m^{-1} K^{-1})	Process	Reference
Organic aerogel			
Polyurethane aerogel	0.017–0.020	Sol-gel and supercritical drying	(Ebert et al., 2021), (Koebel et al., 2017)
Silica aerogel			
Granulate	0.018–0.022	Supercritical drying, freeze-drying or APD	(Borzova et al., 2024), (Gurav et al., 2010b)
Powder	0.020–0.025	Supercritical drying, freeze-drying or APD	(Gurav et al., 2010b), (Liu et al., 2019)
Monolith	0.012–0.014	Supercritical drying, freeze-drying or APD	(Gurav et al., 2010b), ((Koebel et al), (Cheng et al., 2017)
Composites made with silica aerogel			
Mortar	0.029–0.040	Mixing	Gomes et al. (2018)
Slag mortar	0.89–1.32	Mixing	Guzel Kaya and Deveci (2020)
UHPC	0.5–1.00	Mixing	Ng et al. (2015)
Plaster	0.027–0.128	Mixing	Berardi and Nosrati (2018)
Fiber mat (VIP)	0.0147	Mixing in situ and microwave drying	Nocentini et al. (2018)

Currently, the majority of studies around silica aerogel mixed in a composite material evaluate its addition as a filler, used in small quantities. Kim et al. (2015) has investigated a mix of polyvinyl-alcohol and silica aerogel, reducing the thermal conductivity to low values compared to pure PVA, and Ge et al. (2009) have studied epoxy as a binder to both reduce the thermal conductivity and increase the hydrophobicity. Other articles have investigated its adhesiveness to fibers, both synthetic (Talebi et al. (2019)) and natural (Almeida et al. (2021)). The addition of an inorganic matrix such as cement has also been investigated, e.g. Chen et al. (2022) have evaluated the effect of silica aerogel as light particles in cement or concrete.

However, there is room for the development of a composite material where silica aerogel is the main component. Already used in paints (Vanderhoff, 1970), latexes are the main solution when it comes to mixing and binding (small) materials. They are composed of small polymer particles, from 50 nm to 500 nm, in suspension in a liquid medium. Upon application, the liquid evaporates and the polymer particles collapse and form a dense network. Therefore, it traps and maintains all the components that compose the mix, such as stabilizers, pigments, and UV-protective agents. In addition, they are easy to process and do not require specific conditions. Finally, most latex emulsions are now water-based, making them an eco-friendly option for greener manufacturing processes. Combined with the wall cavities filling problematic, latexes could be a promising solution for binding silica aerogel granulates after pumping in the cavities.

Only a few studies have investigated the mix of silica aerogel with latex, and they mainly focused on nano-sized silica aerogel. Yang et al. (2018) have studied the addition of nano-silica fume in latex to evaluate the modification of films' properties. Yet, considering bigger size aerogel, not so many articles investigates a reinforcement without extra filler addition (mainly fibers (Li et al., 2016), (Ul Haq et al., 2017)). Therefore, this study investigates a new strategy based on typical water-based latexes on top of binding enhancement via chemical addition (instead of filler addition) to produce composite materials mainly made with silica aerogel granulates. Key properties such as thermal conductivity and mechanical strength will be evaluated among others like mixing,

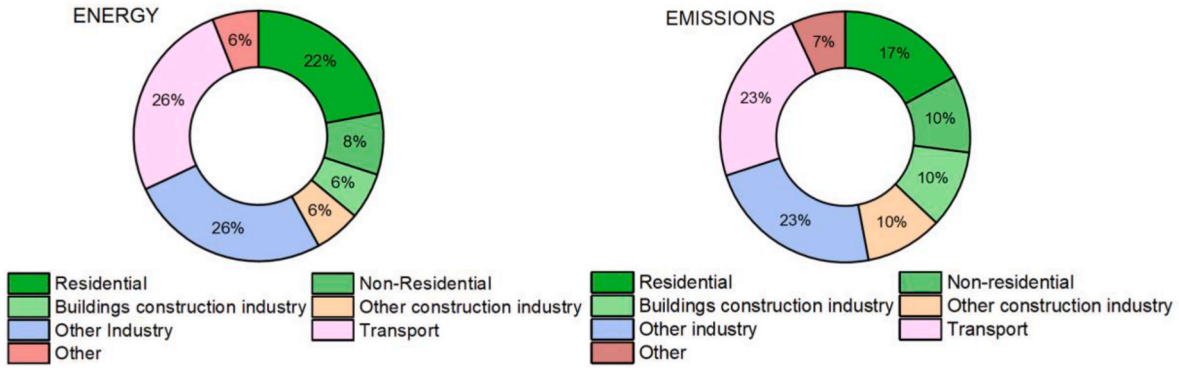

Fig. 1. Shares of energy consumption and CO_2 emissions. Reproduction from "2021 Global Status Report for Buildings and Construction" (a).

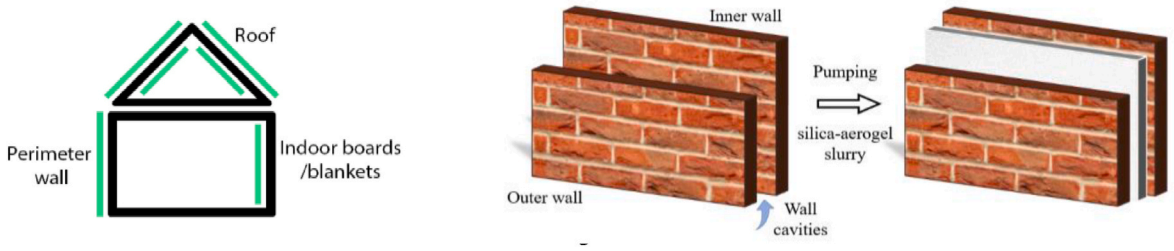

Fig. 2. Examples of building insulations.

thermal stability, and efficiency of the binding. The objective is to offer a thorough comprehension of how binding improvement and composition variations impact thermal insulation capability and mechanical properties.

2. Materials and methods

2.1. Materials

Silica aerogel granulates are from Cabot Corporation, USA (Aerogel Particles P100® – Size from 0.1 to 4.0 mm). Dodecyltriethoxysilane (analytical grade) and absolute ethanol (analytical grade) are purchased from Sigma-Aldrich, Germany. Picassian® AC-122 (40.0 % solid content, water-based, acrylic copolymer emulsion) and Picassian® AC-126 (40.0 % solid content, water-based, styrene-acrylic copolymer emulsion) are kindly provided by Stahl, Netherlands. VINNAPAS® EAF-67 (58.0–62.0 % solid content, water-based, vinyl acetate, ethylene, and acrylate emulsion) is kindly provided by Wacker Chemie, Germany. All chemicals are used without further purification.

2.2. Moisture sorption

Moisture uptakes of the samples are measured in several relative humidities (RH) using saturated salt solutions, i.e. magnesium chloride hexahydrate $MgCl_2.6H_2O$ for 33 % RH, potassium carbonate K_2CO_3 for 43 % RH, sodium bromide NaBr for 59 % RH, sodium chloride NaCl for 75 % RH, potassium chloride KCl for 85 % RH, and potassium sulfate K_2SO_4 for 98 % RH. Before analysis, samples are dried in a desiccator containing silica gel. For each RH, samples are left at least 48 h before the first measurement. After that period, measurements are done every 24 h, until a constant mass is reached.

$$WU = \frac{m_x - m_0}{m_0} * 100 \quad (1)$$

Where m_x stands for the mass at different times, m_0 stands for the initial mass, and WU for water uptake.

2.3. Thermogravimetric analysis – TGA

A thermogravimetric analyzer (TA Instruments TGA Discovery Q5500) is used to investigate the thermal stability of samples. The analysis is done from 30 °C up to 900 °C at 10 °C.min^{-1}. The stability of the samples is assessed by looking at the mass changes due to temperature increases and product evaporation. Before analysis, samples are dried overnight at 50 °C (Memmert universal oven UF260) and crushed to powder afterward. Samples from 5 to 10 mg are prepared for each analysis.

2.4. Thermal conductivity

The transient line source method is used for the measurement of thermal conductivity λ (W m^{-1} K $^{-1}$) by using a hot disk device (AP Isomet model 2104) at room temperature (20 ± 2 °C), with a declared accuracy of 5 % of the reading plus 0.001 W m^{-1} K $^{-1}$. Samples from the procedure described above are tested and λ values are determined. Before the measurement, the samples are dried at 50 °C in an oven (Memmert universal oven UF260) to remove a maximum of water or conditioned in desiccators at various relative humidities (33 %, 43 %, 53 %, 75 %, 85 %, and 98 %), to assess the impact of humidity on the thermal conductivity.

2.5. Particle size distribution – PSD

Size distribution of latexes is measured using a Mastersizer 2000 (Malvern Instrument), with an absorption index of 0.1 and volume concentration of latex close to 0.001 % volume. Size distribution of the commercial aerogel is studied using sieves (2,4 – mechanical sieve (AS 200 control, Retsch), for 2 min with an amplitude of 0,80 mm/"g", to prevent any destruction of the silica aerogel granulates.

2.6. Fourier-transform Infrared Spectroscopy – FT-IR

Samples are analyzed by Fourier-transform Infrared Spectroscopy in

Attenuated total reflection mode (ATR) using a Varian 3100. 20 scans with a resolution of 4 cm^{-1} are effectuated per measurement, from 4000 cm^{-1} to 450 cm^{-1}, in transmittance mode. A background measurement is done before every analysis, and the curves are fitted to the baseline afterward.

2.7. Scanning electron microscopy – SEM

Analyses are performed using a Phenom Pro-X device. Observations are done at different voltages and magnifications, with a backscattered electron detector. Samples are gold coated (Quorum Q150T Plus – 30 mA, coating time = 30 s) before analysis.

2.8. Compression tests

Mechanical strengths of the composite latex/silica aerogel are tested through compression tests, using an MTS Criterion equipped with a load cell of 30 kN at a speed of 2 mm/min, at room temperature. A minimum of 5 samples (30 mm * 30 mm * 10 mm – BS EN 826) are tested for every condition. Measurements are plotted up to 80% displacement.

2.9. Samples processing

2.9.1. Processing conditions

Based on a study by Yang et al. (2018), acrylic latexes are treated with ethanol under magnetic stirring for 5 min. Subsequently, dodecyltriethoxysilane is introduced into the solution and magnetically stirred for 10 min. Then silica aerogel granulates are added to the mix and the mixture is hand-stirred for 5 min until homogenization (Fig. 3).

In this study, extra water will not be added to the mix. Prior tests have shown that the addition of water caused phase separation between the solid part and water, even with significant mixing or a small amount of water, which made it difficult to produce reproducible samples (Fig. 4). As a result, only water-based latexes were used as dispersants, with a ratio solid content/water amount of approximately 50/50, depending on the reference of the latex. This solid content was sufficient to maintain the solution at a suitable level of fluidity, allowing for good stirring and homogenization of the silica aerogel granulates into the emulsion.

Besides, the tests are made only without water, and they differ based on the amount of silica aerogel added. A comprehensive list of all the conducted tests is provided in Table 3. Notably, the T_g of latex 1 and 2 exceeds room temperature, while latex 3's T_g is below room temperature. This variation facilitates evaluation under both conditions.

The samples are shaped using 3D-printed molds (30 * 30 * 10 mm), placed on a thin film, and dried at 50 °C overnight (Memmert universal oven UF260).

2.9.2. Processing characterizations

FTIR spectra are done on crushed samples (raw components and composites) to compare and verify the presence of all the components in the final product (Fig. 5).

The addition of silane in the composites and its efficient dispersion at the interface of the latex particles and the silica aerogel granulates are confirmed by looking at certain peaks: 1390 cm^{-1} and 720 cm^{-1} appeared on the sample made with silane, 950 cm^{-1} is strengthened. The peaks of the different materials are displayed in Table 4. An enlargement of the Si-O-Si at 1060 cm^{-1} from the aerogel is also noticed when the silane is in the mix, with its 1100 cm^{-1} peak. Silane is therefore well integrated into the mix.

In addition to FT-IR measurements, particle size measurements (Fig. 6) are done to observe the effect of the coating of latex particles with the silane. The shifts in particle sizes, from ~0.1 μm to ~ 1 μm, are observed for latexes 1 and 2. On the other side, latex 3 particles are already around 1 μm, no changes are measured.

TGA curves (Fig. 7) exhibit the presence of the silane and how it influences the composites made of silica aerogel and latex. Decomposition temperatures are listed in Table 5.

Composites made with silane present two variations in comparison to the ones without. The first variation happens at around 170 °C, and corresponds to silane decomposition, according to the information provided by the supplier. The second and third mass losses belong to the latexes, from 350 to 400 °C. A shift on the third peak is seen only for latex 2. The second difference appears to be a new degradation, at around 470 °C. Both the shift of latex decomposition and the fourth decomposition could be attributed to the interaction between the silane and the latex. Silane acting as a crosslinker may lead to the formation of a stronger bond between the latex particles and the silica aerogel. This can result in an increase in the thermal stability of the latex and a shift in the degradation temperature. A similar observation was made by mixing silane and fumed silica (Yang et al., 2018). This confirms the observation seen on FTIR (Fig. 5). Hydrogen bonding between the latex particles, coated by the silane and the silica aerogel, is the expected reason of this crosslinking but exact mechanism would require further investigation.

3. Results and discussions

3.1. Structural integrity

A compression machine was employed to test all samples, assessing their response and the reinforcing effect of silane in binding. Results are shown in Fig. 8:

Upon analyzing the samples, a noticeable enhancement in compressive strength is observed when silane is incorporated. The compressive strength of samples without silane appears relatively

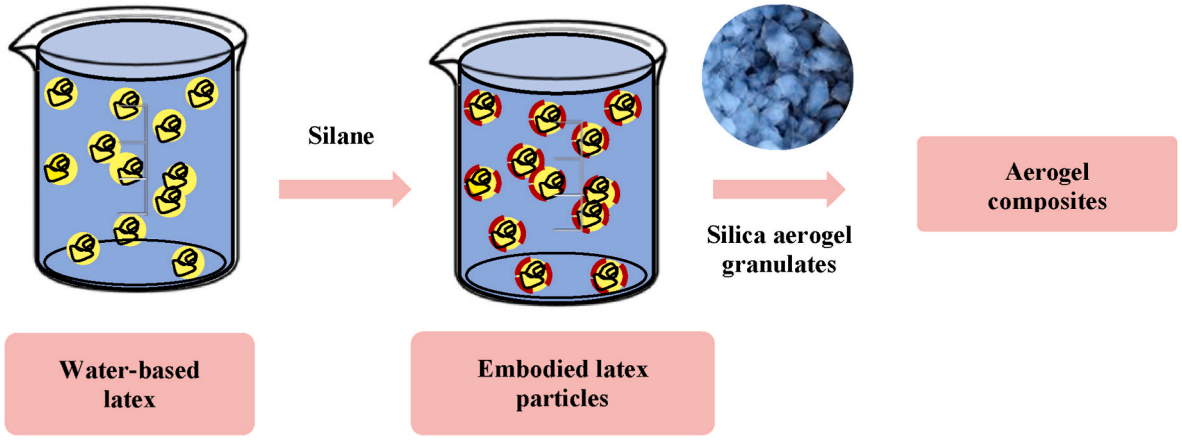

Fig. 3. Process overview.

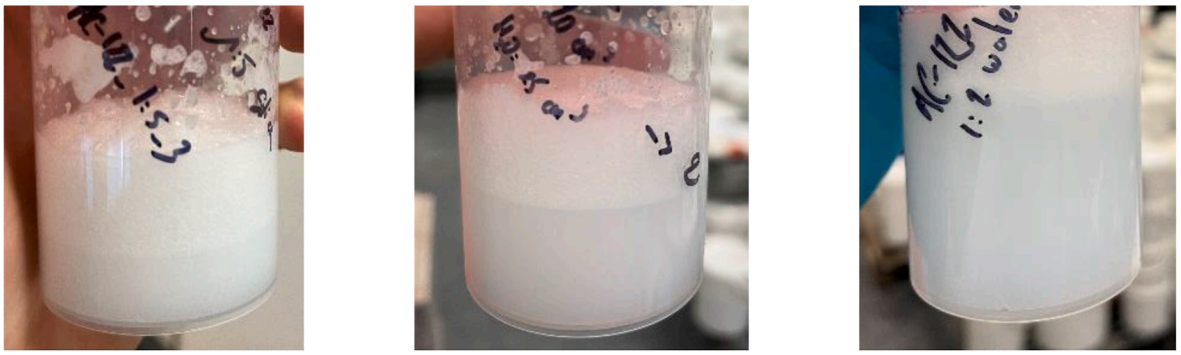

Fig. 4. Samples made with different water amounts.

Table 3
Mix conditions and test labels.

Test	Latex reference	Glass transition (°C)	Ratio (v/v)			Dodecyl-triethoxysilane	Name in the article
			Latex/EtOH	Latex&EtOH/Silane	Silica Aerogel/Silane		
1	Picassian® AC-126	48	5:1	5:1	15:1	No	LC1
2			5:1	5:1	15:1	Yes	LC1-S
3	Picassian® AC-122	35	5:1	5:1	15:1	No	LC2
4			5:1	5:1	15:1	Yes	LC2-S
5	Vinnapas® EAF 67	−35	5:1	5:1	15:1	No	LC3
6			5:1	5:1	15:1	Yes	LC3-S
7	Picassian® AC-126	48	5:1	5:1	22,5:1	No	LC1′
8			5:1	5:1	22,5:1	Yes	LC1′-S

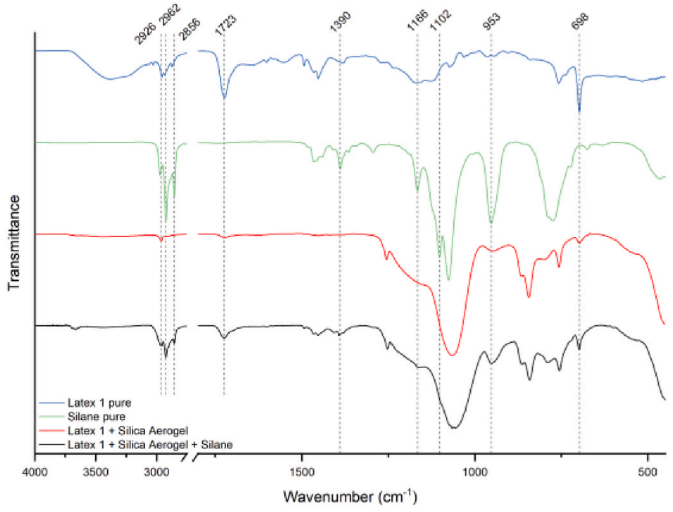

Fig. 5. FTIR comparison of pure silica aerogel, pure silane, latex + silica aerogel, and latex + silica aerogel + silane.

consistent across different T_g values, and so do room temperature behaviors. All the latexes without silane addition exhibit around 0.2 MPa at 40% displacement and 3.5 MPa at 80% displacement. However, distinct improvements are evident with the introduction of silane.

Firstly, looking at the samples made with latex 3, their appearances are close after compression, with or without silane addition. A release of the compression is observed in both conditions but is more important for the samples without silane. The heights remain below the initial one (Fig. 9). The compressive strength at 80% displacement increased by 60%, from 3.58 MPa to 5.78 MPa after silane addition, but it is important to note that the values are similar at 40% and below, being close to 0.2 MPa.

Secondly, for samples made of latexes 1 and 2, a significant transformation is noted in the appearance of compressed samples (Fig. 9).

Table 4
Characteristic absorption peak of FTIR spectrum.

Wavenumber (cm^{-1})	Functional group	Material	References
2966	-CH- from $-CH_3$	Silane & Silica aerogel & Latex	Chen C. et al. (Chen et al., 2015)
2924	-CH- from $-CH_2$	Silane & Silica aerogel & Latex	Chen C. et al. (Chen et al., 2015)
2852	-CH- from $-CH_2$	Silane & Silica aerogel & Latex	Chen C. et al. (Chen et al., 2015)
1721	C=O	Acrylate copolymer (Latex)	
1453	-CO-	Acrylic copolymer (Latex)	
1389	-CO-	Silane	
1253	-*Si*-CH_3	Hydrophobic chains from Silica Aerogel	Chen C. et al. (Chen et al., 2015)
1166	Si-O-C	Silane	
1100	Si-O-C	Silane	Zakirov A. et al. (Zakirov et al., 2007)
1080	Si-O-Si	Silane	Chen C. et al. (Chen et al., 2015)
1060	Si-O-Si	Silica Aerogel	
950	Si-O(H)	Silane & Silica Aerogel	Lenza R. et al. (Chen et al., 2015)
850	Si-CH	Hydrophobic chains from Silica Aerogel	Chen C. et al. (Chen et al., 2015)
750	Si-O	Silica Aerogel	
723	$-CH_2$-	Silane	
700	-CH- from benzene	Latex	

Without silane, all tested samples exhibit a crumbly aspect after compression, showing a complete collapse of the composite's structure. This behavior is attributed to the T_g of the latex. Latex 3, with a T_g lower than room temperature, displays greater flexibility, while latexes 1 and 2, with a T_g above room temperature, lead to their brittle response. Additionally, the samples made without silane bounce back after compression release (Fig. 9 - d). On the opposite, samples with added silane maintain their compressed height, showcasing a compact and

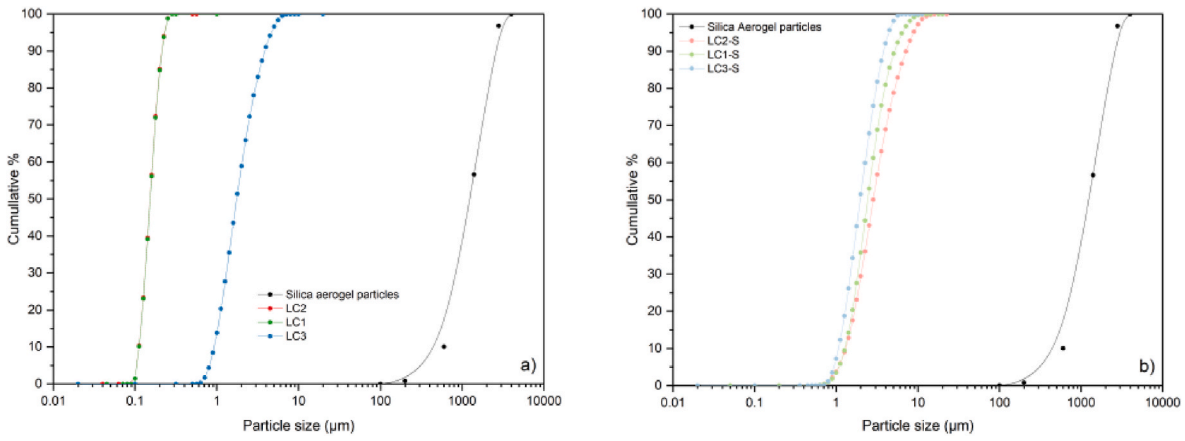

Fig. 6. Particle size distribution of latex emulsions without (a) and with silane (b).

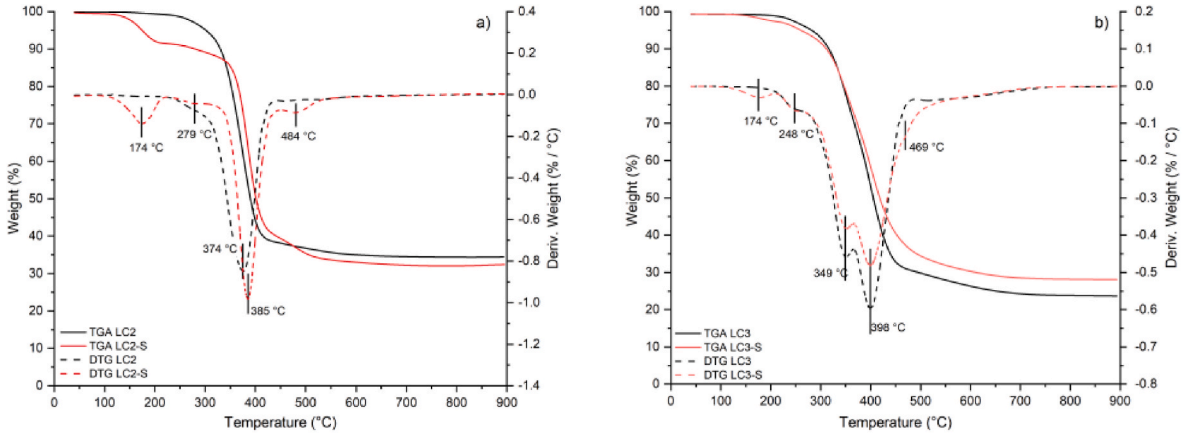

Fig. 7. TGA and DTG curves for latex 2 (a) and latex 3 (b).

Table 5
Decomposition temperatures from the DTG curves.

Names	T (°C) 1st deg.	T (°C) 2nd deg.	T (°C) 3rd deg.	T (°C) 4th deg.
LC1-S	162	/	374	450
LC1	/	/	374	/
LC2-S	177	279	387	484
LC2	/	279	379	/
LC3-S	174	248	349 + 398	469
LC3	/	248	349 + 398	/

stable appearance (Fig. 9 – b). These observed responses are attributed to a more robust bonding between all the components, caused by the addition of silane. This accounts for the observed improvements in compressive strength and structural integrity. This enhancement is even more pronounced for samples made with latexes 1 and 2. Responses at 80% displacement are almost six times more important, from 3.66 MPa to 23.84 MPa, and three times more important, shifting from 4.20 MPa to 12.27 MPa, for latexes 1 and 2, respectively. The same trend is observed also at lower displacements, where the shifts at 40% displacement increase by almost six times (from 0.16 to 0.91 MPa) and two times (from 0.23 to 0.58 MPa) and for latexes 1 and 2, respectively.

The samples were observed under SEM (Fig. 10).

SEM images of the silica aerogel granulates reveal that the addition of silane results in a rougher surface texture, characterized by a higher concentration of small particles on their surfaces. Corroborating these results with the ones from the compression tests, it becomes evident that the presence of silane enhances the bonding within the silica aerogel structure.

Contrarywise, no differences can be seen on the micrographs of the latex 3 samples (Fig. 11). The stretched latex part on both of them comes from the latex 3 having at T_g below the room temperature, and no differences can be seen on the aspect of the silica aerogel granulates from the SEM images.

Analyzing the outcomes of the compression tests and SEM pictures, latexes with a T_g exceeding room temperature emerge as a more suitable option for insulation needs. Flexibility is not essential as the composites adopt the application's forms, and these composites yield the most favorable binding enhancement results.

3.2. *Thermal conductivity behavior*

The thermal conductivities of the samples are depicted in Fig. 12.

From these results, latex 1 demonstrates the most effective thermal insulation, while latex 3 exhibits the highest thermal conductivity. The difference is quite significant, with values nearly tripling between the two extremes - from 0.022 W m^{-1} K^{-1} for latex 1 to 0.066 W m^{-1} K^{-1} for latex 3. Latex 3 values (0.052 W m^{-1} K^{-1} and 0.066 W m^{-1} K^{-1}), along with latex 2 with silane to some extent (0.039 W m^{-1} K^{-1}), fall short in comparison to established thermal insulation benchmarks as seen in Table 2, where the most efficient ones come close to 0.015 W m^{-1} K^{-1} for silica aerogel alone, and around 0.030 W m^{-1} K^{-1} for commercially available products.

Interestingly, the addition of silane does not appear to enhance thermal insulation. It leads to a decrease in the thermal properties of

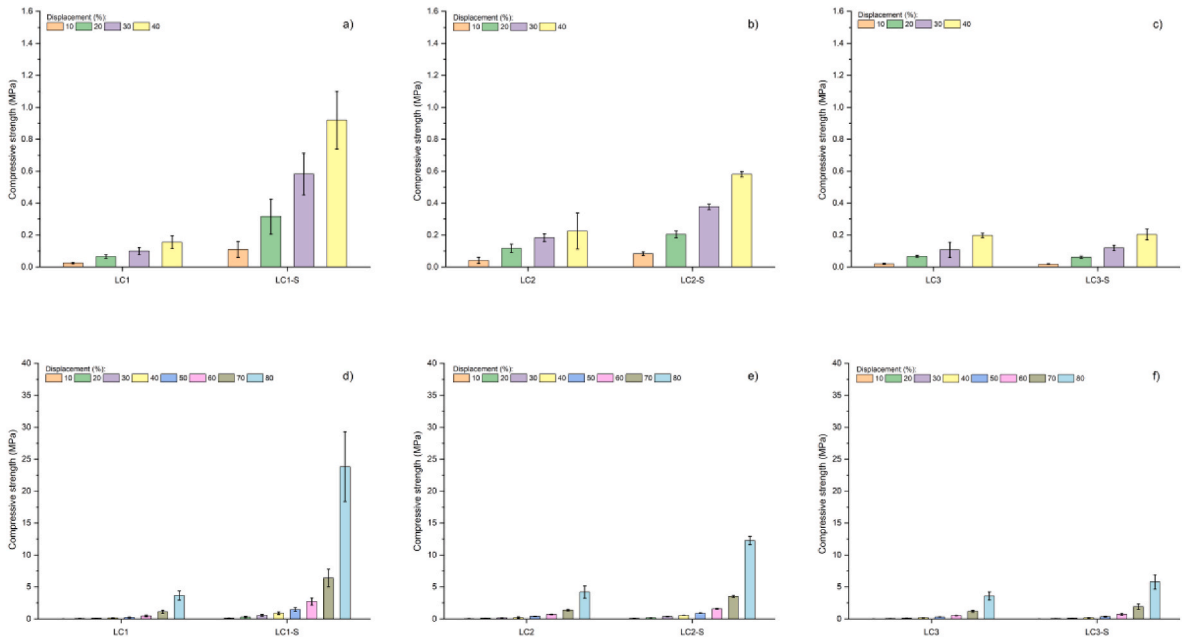

Fig. 8. Impact of the silane on compression tests: Displacements up to 40% - a), b) and c), and full displacements - d), e) and f).

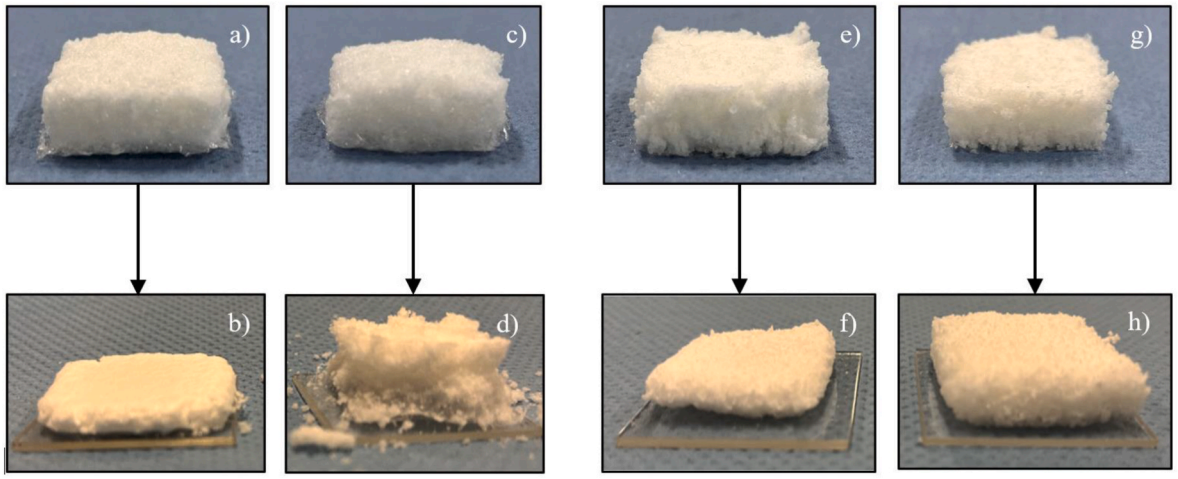

Fig. 9. Samples before/after compression: a) Latex 1 + silane before, b) Latex 1 + silane after, c) Latex 1 no silane before, d) Latex 1 no silane after, e) Latex 3 + silane before, f) Latex 3 + silane after, g) Latex 3 no silane before, h) Latex 3 no silane.

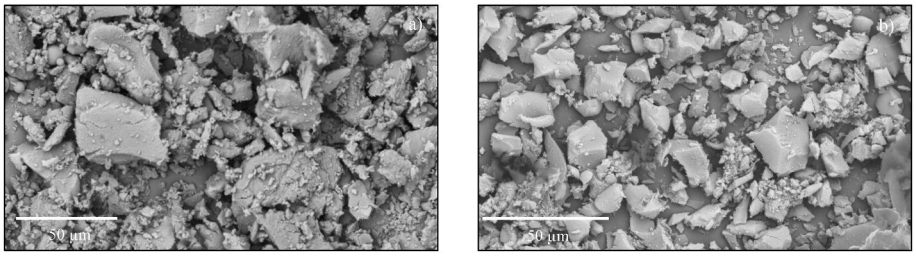

Fig. 10. SEM pictures of crushed samples: a) Latex 1 + silane, b) Latex 1 no silane.

latex 2 and 3, from 0.030 W m^{-1} K^{-1} to 0.039 W m^{-1} K^{-1} and 0.052 W m^{-1} K^{-1} to 0.067 W m^{-1} K^{-1}, respectively. Only a marginal improvement is observed for latex 1, where values shift from 0.031 W m^{-1} K^{-1} to 0.022 W m^{-1} K^{-1}. Hence, despite the relatively small proportion of latexes in the composites, any small modifications or perturbations significantly affect the thermal properties of the composites. Regarding the impact of T_g on thermal conductivity in polymers, Dos Santos et al. (Dos Santos et al., 2013) have demonstrated a relationship between T_g, thermal conductivity, and the temperature of the analysis. This correlation is evident in this study, especially with latex 2 having a T_g value closer to room temperature than latex 1.

Overall, factors such as atomic composition and chemical structure

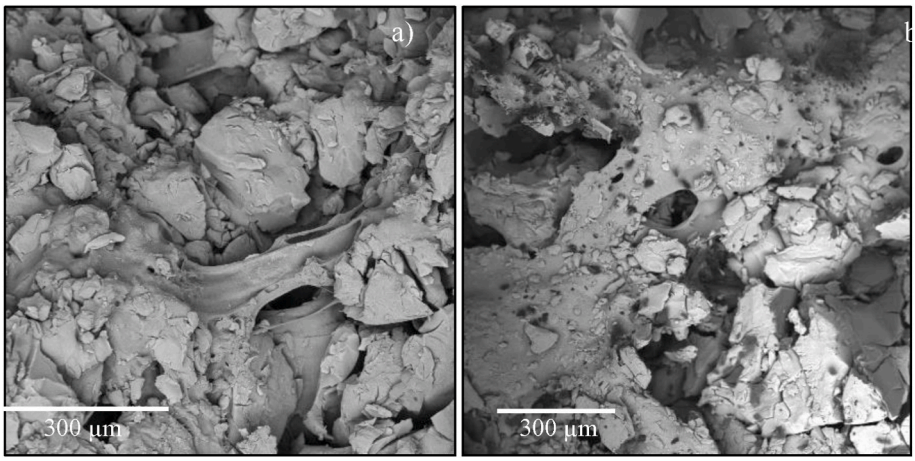

Fig. 11. SEM pictures of crushed samples: a) Latex 3 + silane, b) Latex 1 no silane.

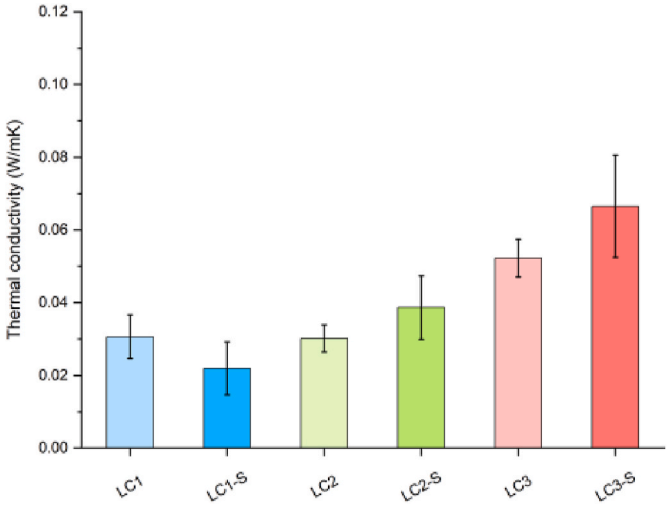

Fig. 12. Thermal conductivity of the different latex composites.

might influence thermal conductivity, as suggested by Zhang et al. (2014), therefore, it would necessitate further investigation for deeper understanding to find the perfect latex with the lowest thermal conductivity. Additionally, it might be interesting to point out that latex 3's composites have both the worst thermal conductivity and the lowest mechanical resistance. But, if a correlation exists, it will need deeper evaluation to assess it.

Continuing the sample analysis, it is essential to assess moisture absorption. Belkharchouche et al. (Belkharchouche and Chaker, 2016) and Hong-Qing et al. (Jin et al., 2016) have highlighted the influence of moisture sorption on thermal conductivity.

In Fig. 13, the relationship between weight and relative humidity is presented. Especially, the samples display minimal moisture absorption, in line with the hydrophobic nature of both the latexes and silica aerogel granulates. The highest increase is observed for latex 1 made without silane, reaching 1.58 m% at 98% r.h. Moreover, a general trend emerges where the addition of silane decreases the moisture sorption compared to samples without it. The presence of silane strengthens binding, subsequently increasing hydrophobicity.

After accounting for the modest yet present moisture sorption, the thermal conductivity was assessed at various relative humidities (as shown in Fig. 13). The thermal conductivity values exhibit sensitivity to rising moisture content within the samples, as evidenced by a proportional increase in thermal conductivity with the absorbed moisture. The biggest change is observed for the sample composed of latex 3 with additional silane, which shifts from 0.067 W m^{-1} K^{-1} in a dry state to 0.087 W m^{-1} K^{-1} at 98% r.h.

3.3. Silica aerogel to latex ratio

To assess the influence of composite material quantity, distinct compositions were created, both with and without silane, to analyze the variations in previously assessed properties. Latex 1, which has the best thermal conductivity results, was chosen to assess the differences when the ratio of silica aerogel to latex is modified. The moisture absorption results are illustrated in Fig. 14.

The main distinction is that the presence of silane does not affect the weight fluctuations as the silica aerogel amount increases. Overall, moisture sorption remains minimal, with the highest increase observed at 1.58 m% for the silica-to-latex ratio of 15:1, occurring at 98 % r.h.

As depicted in Fig. 14, the thermal conductivity trends of the samples in relation to varying relative humidities mirror those observed in samples made using different latexes. The minor weight fluctuations noted earlier again lead to an increase in thermal conductivity values. The most consistent outcomes are observed in samples with a lower latex-to-silica aerogel ratio. Specifically, their thermal conductivities range from 0.032 W m^{-1} K^{-1} to 0.038 W m^{-1} K^{-1} with silane, and from 0.028 W m^{-1} K^{-1} to 0.033 W m^{-1} K^{-1} without silane.

This trend is even more pronounced in samples with a 22.5:1 ratio, exhibiting a larger increase in thermal conductivity. With the inclusion of silane, thermal conductivity rises from 0.070 W m^{-1} K^{-1} to 0.086 W m^{-1} K^{-1}, and without silane, it increases from 0.043 W m^{-1} K^{-1} to 0.051 W m^{-1} K^{-1}. However, an intriguing observation is made when the amount of silica aerogel increases. Contrary to the expected notion that greater silica aerogel content, being a thermal insulator material, would lead to decreased thermal conductivity or at least maintain it within a similar range, results demonstrate the opposite. The thermal conductivity values in this scenario are unexpectedly high, which is a counterintuitive finding.

A plausible explanation could be attributed to the distribution of the materials within the sample. In the 15:1 ratio, a larger proportion of latex is present, which can readily occupy interstices between the relatively larger silica aerogel granulates (Fig. 6). On the contrary, a lower latex content could result in a higher amount of voids within the samples, incapable of being filled by silica aerogel granulates due to their size. These additional empty spaces might unfavorably impact thermal conductivity, contributing to the observed rise in values. Another reason could be the difficulty to mix homogeneously the silica aerogel and the latex, because of the amount of silica aerogel.

In Fig. 15, the disparity in compressive strengths between the two ratios is displayed. Firstly, the impact of the silane addition is important

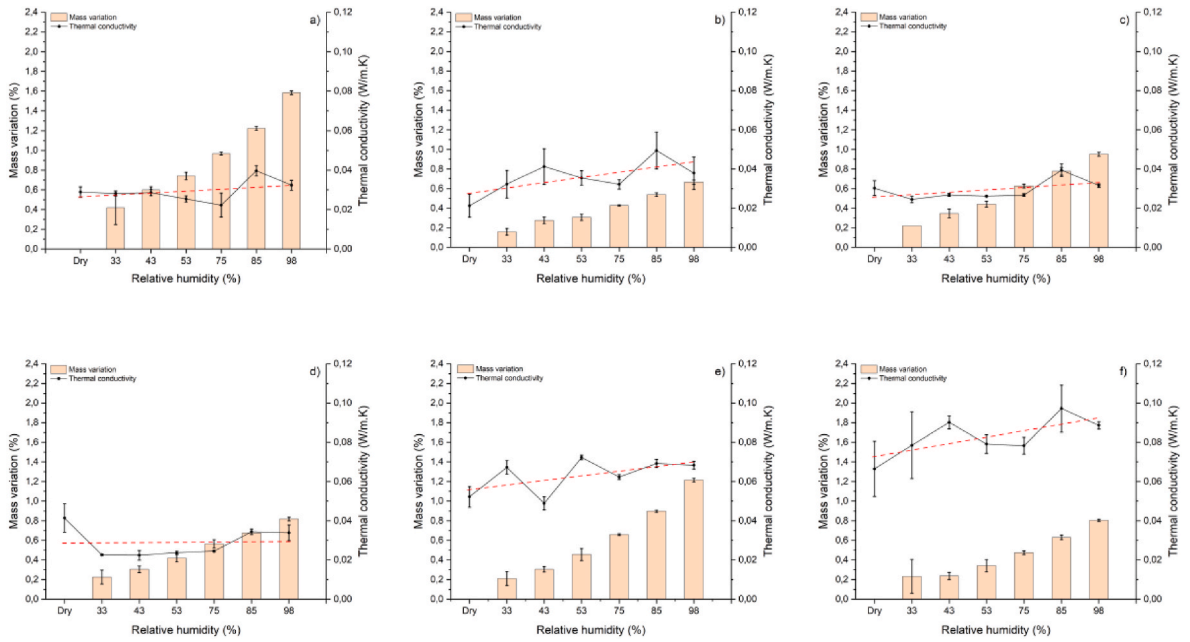

Fig. 13. Weight variations and thermal conductivities regarding relative humidity - a) Latex 1 without silane b) Latex 1 with silane c) Latex 2 without silane d) Latex 2 with silane e) Latex 3 without silane f) Latex 3 with silane. Dashed lines are the fitted curves of the thermal conductivity measurements.

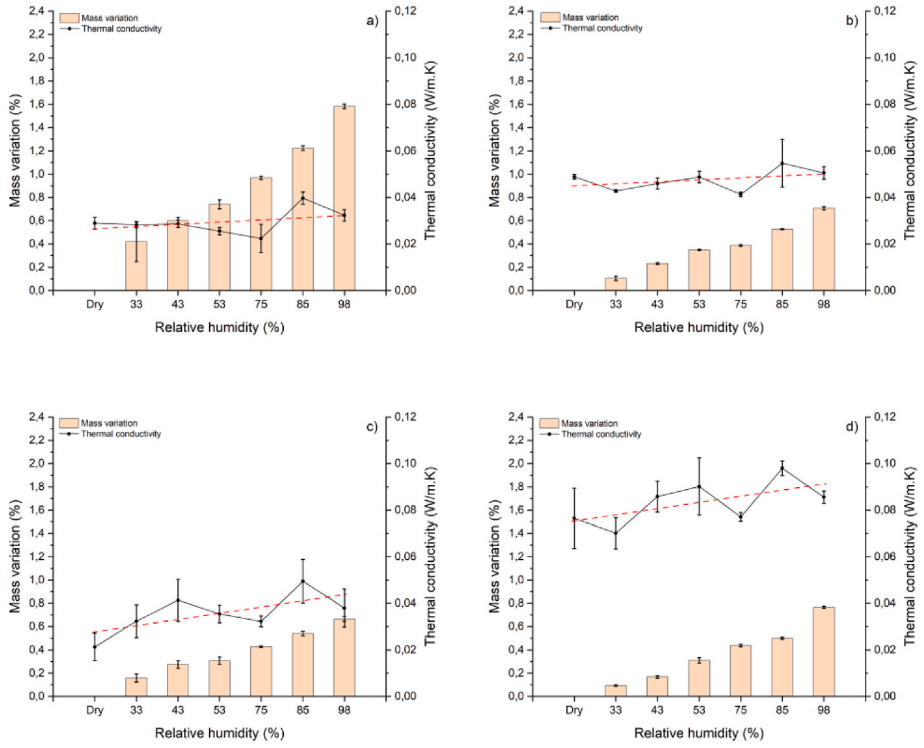

Fig. 14. Weight variations and thermal conductivity values regarding relative humidity - a) Ratio 15:1 without silane b) Ratio 22,5:1 without silane c) Ratio 15:1 with silane d) Ratio 22,5:1 with silane. Dashed lines are the fitted curves of the thermal conductivity measurements.

in the initial displacements, up to 40%, regardless of the ratio. For instance, at 40% displacement for latex 1′, the compressive strength rises over tenfold, from 0.049 MPa to 0.79 MPa, when silane is incorporated. Secondly, at the 22.5:1 ratio, the samples without silane exhibit a more pronounced collapse (Fig. 16). This result can be observed on the compression strength values, where the increase in silica aerogel amount leads to a decrease in the compressive response, shifting from 23.84 MPa to 10.52 MPa, at 80% displacement. The same trend is observed at lower displacements.

4. Conclusions

This study evaluates the manufacture of silica-aerogel composites with various latexes as a matrix also enhanced by the use of a silane coupling agent. The objectives of this study were to assess the effectiveness of chemical binding reinforcement and the resulting effect on

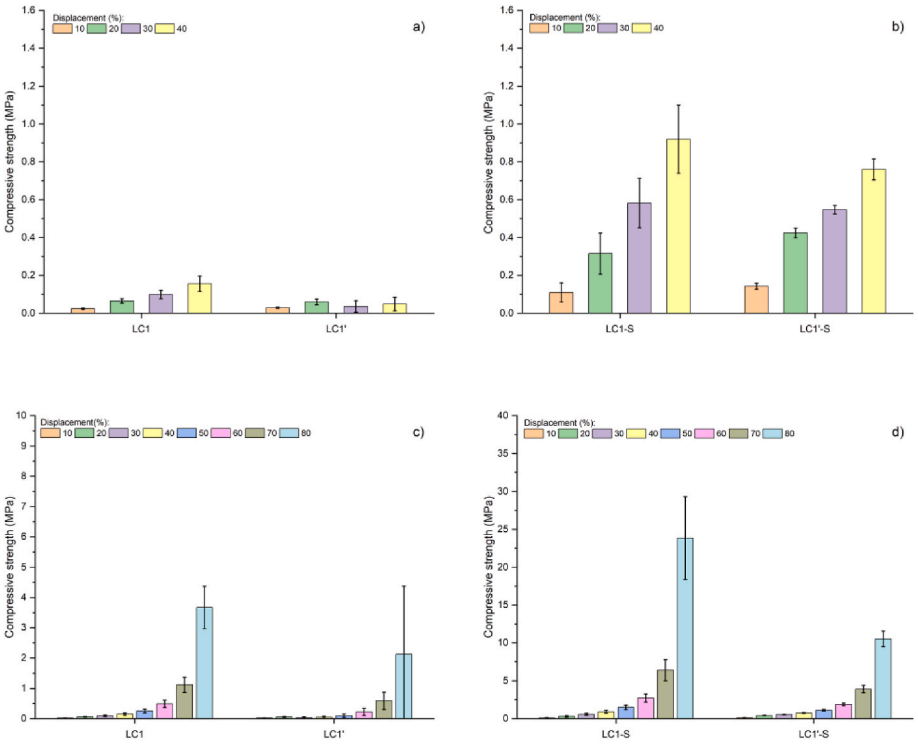

Fig. 15. Compression tests, effect of the ratio: Up to 40% - a) and b), and full displacements - c) and d).

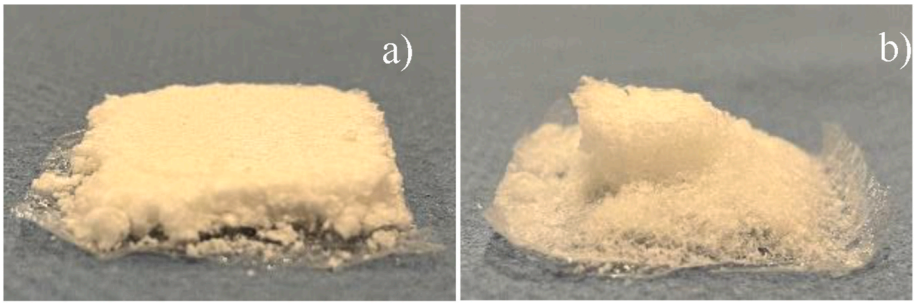

Fig. 16. 22.5:1 samples after compression - a) with silane, b) without silane.

the thermal conductivity of the composites. Upon examining the findings, several key trends emerge:

Primarily, across all samples, silica aerogel keeps the higher impact on the thermal conductivity, leading to values around 0.02/0.03 W m^{-1} K^{-1}. These values are only slightly higher than the silica aerogel (Monolithic - 0.012 W m^{-1} K^{-1}). Additionally, the incorporation of a silane for binding enhancement not only increases the mechanical properties but also enhances the material's physical response. This leads to a more cohesive composite, reducing crumbliness and improving the overall quality of the material.

Moreover, the behavior against outdoor conditions is also studied, and the results show that, even at high relative humidity, the absorption remains very low for all the samples. But, in the meantime, even a low moisture sorption impacts all the samples and has a non-negligible impact on the thermal conductivity.

Based on these results, here are the most important parameters to take into account to maximize the properties of latex-aerogel composites.

- Identifying the most suitable latex among available options tailored to specific application conditions,
- Further reduction in water usage, especially for the latex,
- Fine-tuning the composite's composition to increase silica-aerogel content while maintaining acceptable processing conditions and mechanical properties.

This work promotes the development of silica aerogel applications, particularly in housing refurbishing, where addressing energy efficiency and enhancing indoor quality remains a persistent challenge.

CRediT authorship contribution statement

Samuel Pantaleo: Writing – review & editing, Writing – original draft, Methodology, Investigation, Conceptualization. **Florent Gauvin:** Writing – review & editing, Supervision. **Katrin Schollbach:** Writing – review & editing, Supervision. **H.J.H. Brouwers:** Writing – review & editing, Supervision.

Declaration of competing interest

The authors declare that they have no known competing financial interests or personal relationships that could have appeared to influence the work reported in this paper.

Data availability

Data will be made available on request.

References

2021 Global Status Report for Buildings and Construction | UNEP - UN Environment Programme, [Online]. Available:."Accessed: April. 14, 2023. https://www.unep.org/resources/report/2021-global-status-report-buildings-and-construction.

Abu-Jdayil, B., Mourad, A.H., Hittini, W., Hassan, M., Hameedi, S., 2019. Traditional, state-of-the-art and renewable thermal building insulation materials: an overview. Constr Build Mater 214, 709–735. https://doi.org/10.1016/J.CONBUILDMAT.2019.04.102.

Almeida, C.M.R., Ghica, M.E., Ramalho, A.L., Durães, L., 2021. Silica-based aerogel composites reinforced with different aramid fibres for thermal insulation in Space environments. J. Mater. Sci. 56 (24), 13604–13619. https://doi.org/10.1007/S10853-021-06142-3/TABLES/6.

The Netherlands 2020 – Analysis - IEA."Accessed: May 3, 2023. [Online]. Available: https://www.iea.org/reports/the-netherlands-2020.

Belkharchouche, D., Chaker, A., 2016. Effects of moisture on thermal conductivity of the lightened construction material. Int. J. Hydrogen Energy 41 (17), 7119–7125. https://doi.org/10.1016/J.IJHYDENE.2016.01.160.

Berardi, U., 2017. A cross-country comparison of the building energy consumptions and their trends. Resour. Conserv. Recycl. 123, 230–241. https://doi.org/10.1016/J.RESCONREC.2016.03.014.

Berardi, U., Nosrati, R.H., 2018. Long-term thermal conductivity of aerogel-enhanced insulating materials under different laboratory aging conditions. Energy 147, 1188–1202. https://doi.org/10.1016/J.ENERGY.2018.01.053.

Berger, F., Gauvin, F., Brouwers, H.J.H., 2020. The recycling potential of wood waste into wood-wool/cement composite. Constr Build Mater 260, 119786. https://doi.org/10.1016/J.CONBUILDMAT.2020.119786.

Bin Rashid, A., et al., 2023. Silica aerogel: synthesis, characterization, applications, and Recent Advancements. Part. Part. Syst. Char. 40 (6), 2200186. https://doi.org/10.1002/PPSC.202200186.

Borzova, M., Schollbach, K., Gauvin, F., Brouwers, H.J.H., 2024. Sustainable ambient pressure-dried silica aerogel from waste glass. Current Research in Green and Sustainable Chemistry 9, 100425. https://doi.org/10.1016/J.CRGSC.2024.100425.

Bozsaky, D., 2010. The historical development of thermal insulation materials. Periodica Polytechnica Architecture 41 (2), 49–56. https://doi.org/10.3311/PP.AR.2010-2.02.

Chen, C., Jia, Z., Wang, X., Lu, H., Guan, Z., Yang, C., 2015. Micro characterization and degradation mechanism of liquid silicone rubber used for external insulation. IEEE Trans. Dielectr. Electr. Insul. 22 (1), 313–321. https://doi.org/10.1109/TDEI.2014.004188.

Chen, Y.X., Hendrix, Y., Schollbach, K., Brouwers, H.J.H., 2020. A silica aerogel synthesized from olivine and its application as a photocatalytic support. Constr Build Mater 248, 118709. https://doi.org/10.1016/J.CONBUILDMAT.2020.118709.

Chen, Y.X., Klima, K.M., Brouwers, H.J.H., Yu, Q., 2022. Effect of silica aerogel on thermal insulation and acoustic absorption of geopolymer foam composites: the role of aerogel particle size. Compos. B Eng. 242, 110048. https://doi.org/10.1016/J.COMPOSITESB.2022.110048.

Cheng, X., Li, C., Shi, X., Li, Z., Gong, L., Zhang, H., 2017. Rapid synthesis of ambient pressure dried monolithic silica aerogels using water as the only solvent. Mater. Lett. 204, 157–160. https://doi.org/10.1016/J.MATLET.2017.05.107.

Chruściel, J.J., Leśniak, E., 2015. Modification of epoxy resins with functional silanes, polysiloxanes, silsesquioxanes, silica and silicates. Prog. Polym. Sci. 41, 67–121. https://doi.org/10.1016/J.PROGPOLYMSCI.2014.08.001.

Chun, C., Kwok, A., Mitamura, T., Miwa, N., Tamura, A., 2008. Thermal diary: Connecting temperature history to indoor comfort. Build. Environ. 43 (5), 877–885. https://doi.org/10.1016/J.BUILDENV.2007.01.031.

Doroudiani, S., Kortschot, M.T., 2003. Polystyrene foams. I. Processing-structure relationships. J. Appl. Polym. Sci. 90 (5), 1412–1420. https://doi.org/10.1002/APP.12804.

Dos Santos, W.N., De Sousa, J.A., Gregorio, R., 2013. Thermal conductivity behaviour of polymers around glass transition and crystalline melting temperatures. Polym. Test. 32 (5), 987–994. https://doi.org/10.1016/J.POLYMERTESTING.2013.05.007.

Ebert, H.P., et al., 2021. Intercomparison of thermal conductivity measurements on a Nanoporous organic aerogel. Int. J. Thermophys. 42 (2), 1–18. https://doi.org/10.1007/S10765-020-02775-9/FIGURES/15.

Gauvin, F., Tsao, V., Vette, J., Brouwers, H.J.H., 2022. Physical properties and hygrothermal behavior of mycelium-based composites as foam-like wall insulation material. Bio-Based Building Materials 1, 643–651. https://dx.doi.org/10.4028/www.scientific.net/cta.1.643.

Ge, D., Yang, L., Li, Y., Zhao, J.P., 2009. Hydrophobic and thermal insulation properties of silica aerogel/epoxy composite. J. Non-Cryst. Solids 355 (52–54), 2610–2615. https://doi.org/10.1016/J.JNONCRYSOL.2009.09.017.

Gomes, M.G., Flores-Colen, I., da Silva, F., Pedroso, M., 2018. Thermal conductivity measurement of thermal insulating mortars with EPS and silica aerogel by steady-state and transient methods. Constr Build Mater 172, 696–705. https://doi.org/10.1016/J.CONBUILDMAT.2018.03.162.

Grazieschi, G., Asdrubali, F., Thomas, G., 2021. Embodied energy and carbon of building insulating materials: a critical review. Cleaner Environmental Systems 2, 100032. https://doi.org/10.1016/J.CESYS.2021.100032.

Gurav, J.L., Jung, I.K., Park, H.H., Kang, E.S., Nadargi, D.Y., 2010a. Silica aerogel. J. Nanomater. 2010, 11. https://doi.org/10.1155/2010/409310.

Gurav, J.L., Jung, I.K., Park, H.H., Kang, E.S., Nadargi, D.Y., 2010b. Silica aerogel: synthesis and applications. J. Nanomater. 2010 (1), 409310. https://doi.org/10.1155/2010/409310.

Guzel Kaya, G., Deveci, H., 2020. Synergistic effects of silica aerogels/xerogels on properties of polymer composites: a review. J. Ind. Eng. Chem. 89, 13–27. https://doi.org/10.1016/J.JIEC.2020.05.019.

Hammond, G., Jones, C., 2008. INVENTORY of CARBON & ENERGY (ICE) Version 1.6a [Online]. Available: www.bath.ac.uk/mech-eng/sert/embodied/. (Accessed 8 May 2024).

Jelle, B.P., Mofid, S.A., Gao, T., Grandcolas, M., Sletnes, M., Sagvolden, E., 2019. Nano insulation materials exploiting the Knudsen effect. IOP Conf. Ser. Mater. Sci. Eng. 634 (1), 012003. https://doi.org/10.1088/1757-899X/634/1/012003.

Jensen, L., 2020. EU climate target plan – Raising the level of ambition for 2030. Climate Action Research and Tracking Service, Members' Research Service PE 659, 370.

Jin, H.Q., Yao, X.L., Fan, L.W., Xu, X., Yu, Z.T., 2016. Experimental determination and fractal modeling of the effective thermal conductivity of autoclaved aerated concrete: effects of moisture content. Int J Heat Mass Transf 92, 589–602. https://doi.org/10.1016/J.IJHEATMASSTRANSFER.2015.08.103.

Khudeev, I.I., Lebedev, A.E., Mochalova, M.S., Menshutina, N.V., 2024. Modeling and techno-economic optimization of the supercritical drying of silica aerogels. Dry. Technol. 42 (5), 812–835. https://doi.org/10.1080/07373937.2024.2318439.

Kim, H.M., Noh, Y.J., Yu, J., Kim, S.Y., Youn, J.R., 2015. Silica aerogel/polyvinyl alcohol (PVA) insulation composites with preserved aerogel pores using interfaces between the superhydrophobic aerogel and hydrophilic PVA solution. Compos Part A Appl Sci Manuf 75, 39–45. https://doi.org/10.1016/J.COMPOSITESA.2015.04.014.

M. Koebel, A. Rigacci, and P. Achard, "Aerogel-based Thermal Superinsulation: an Overview",doi: 10.1007/s10971-012-2792-9.

Koebel, M.M., Wernery, J., Malfait, W.J., 2017. Energy in buildings—Policy, materials and solutions. MRS Energy & Sustainability 4 (1). https://doi.org/10.1557/MRE.2017.14.

Koh, C.H., Gauvin, F., Schollbach, K., Brouwers, H.J.H., 2022. Investigation of material characteristics and hygrothermal performances of different bio-based insulation composites. Constr Build Mater 346, 128440. https://doi.org/10.1016/J.CONBUILDMAT.2022.128440.

Lamb, W.F., et al., 2021. A review of trends and drivers of greenhouse gas emissions by sector from 1990 to 2018. Environ. Res. Lett. 16 (7), 073005. https://doi.org/10.1088/1748-9326/ABEE4E.

Li, Z., Cheng, X., He, S., Shi, X., Gong, L., Zhang, H., 2016. Aramid fibers reinforced silica aerogel composites with low thermal conductivity and improved mechanical performance. Compos Part A Appl Sci Manuf 84, 316–325. https://doi.org/10.1016/J.COMPOSITESA.2016.02.014.

Li, C., et al., 2023. Silica aerogels: from materials research to industrial applications. Int. Mater. Rev. https://doi.org/10.1080/09506608.2023.2167547/SUPPL_FILE/YIMR_A_2167547_SM6531.ZIP.

Lin, P., Mah, M., Randi, J., DeFrances, S., Bernot, D., Talghader, J.J., 2023. High average power optical properties of silica aerogel thin film. Thin Solid Films 768, 139722. https://doi.org/10.1016/J.TSF.2023.139722.

Liu, R., Wang, J., Du, Y., Liao, J., Zhang, X., 2019. Phase-separation induced synthesis of superhydrophobic silica aerogel powders and granules. J. Solid State Chem. 279, 120971. https://doi.org/10.1016/J.JSSC.2019.120971.

Mermer, N.K., Piskin, S., 2018. Silica based aerogel synthesis from fly ash and bottom ash: the effect of synthesis parameters on the structure. Main Group Chem. 17 (1), 63–77. https://doi.org/10.3233/MGC-180254.

Ng, S., Jelle, B.P., Sandberg, L.I.C., Gao, T., Wallevik, Ó.H., 2015. Experimental investigations of aerogel-incorporated ultra-high performance concrete. Constr Build Mater 77, 307–316. https://doi.org/10.1016/J.CONBUILDMAT.2014.12.064.

Nocentini, K., Achard, P., Biwole, P., 2018. Hygro-thermal properties of silica aerogel blankets dried using microwave heating for building thermal insulation. Energy Build. 158, 14–22. https://doi.org/10.1016/J.ENBUILD.2017.10.024.

Papadopoulos, A.M., 2005. State of the art in thermal insulation materials and aims for future developments. Energy Build. 37 (1), 77–86. https://doi.org/10.1016/J.ENBUILD.2004.05.006.

F. Soghra Jahed, S. Hamidi, M. Zamani-Kalajahi, and M. Siahi-Shadbad, "Biomedical applications of silica-based aerogels: a comprehensive review," Macromol. Res., vol.31, pp. 519–538, doi: 10.1007/s13233-023-00142-9.

Talebi, Z., Soltani, P., Habibi, N., Latifi, F., 2019. Silica aerogel/polyester blankets for efficient sound absorption in buildings. Constr Build Mater 220, 76–89. https://doi.org/10.1016/J.CONBUILDMAT.2019.06.031.

Ul Haq, E., Zaidi, S.F.A., Zubair, M., Abdul Karim, M.R., Padmanabhan, S.K., Licciulli, A., 2017. Hydrophobic silica aerogel glass-fibre composite with higher strength and thermal insulation based on methyltrimethoxysilane (MTMS) precursor. Energy Build. 151, 494–500. https://doi.org/10.1016/J.ENBUILD.2017.07.003.

Vanderhoff, J.W., 1970. Mechanism of film formation of latices. Br. Polym. J. 2 (3), 161–173. https://doi.org/10.1002/PI.4980020301.

Volk, R., et al., 2024. Life cycle assessment of mycelium-based composite materials. Resour. Conserv. Recycl. 205, 107579. https://doi.org/10.1016/J.RESCONREC.2024.107579.

Yang, J., et al., 2018. Facile Fabrication of superhydrophobic Nanocomposite coatings based on water-based emulsion latex. Adv Mater Interfaces 5 (15), 1800207. https://doi.org/10.1002/ADMI.201800207.

Zakirov, A.S., et al., 2007. Comparative study on the structural and Electrical properties of low-bftextitk SiOC(-H) films Deposited by using Plasma enhanced chemical Vapor Deposition Comparative study on the structural and Electrical properties of low-k

SiOC(-H) films Deposited by U. J. Kor. Phys. Soc. 50 (6), 1809–1813. https://doi.org/10.3938/jkps.50.1809.
Zhang, H., Arens, E., Pasut, W., 2011. Air Temperature Thresholds for Indoor Comfort and Perceived Air Quality, vol. 39, pp. 134–144. https://doi.org/10.1080/09613218.2011.552703, 2.
Zhang, T., Wu, X., Luo, T., 2014. Polymer nanofibers with outstanding thermal conductivity and thermal stability: Fundamental linkage between molecular characteristics and macroscopic thermal properties. J. Phys. Chem. C 118 (36), 21148–21159. https://doi.org/10.1021/JP5051639/ASSET/IMAGES/LARGE/JP-2014-051639_0011.JPEG.
A. [D-N.-14] Rep. Ocasio-Cortez, 2019. Text - H.Res.109 - 116th Congress (2019-2020): Recognizing the Duty of the Federal Government to Create a Green New Deal [Online]. Available: https://www.congress.gov/bill/116th-congress/house-resolution/109/text. (Accessed 17 October 2024).
Core insulation materials – optiDämm."Accessed: October. 17, 2024. [Online]. Available: https://www.optidaemm.de/waermedaemmung/daemmstoffe/kerndaemmstoffe.
Produit - Gramitherm. https://gramitherm.eu/produits/. (Accessed 18 October 2024).
Rénovation énergétique." Accessed: October. 17, 2024. [Online]. Available: https://www.ecologie.gouv.fr/politiques-publiques/savoir-renovation-energetique.
SLENTITE®." Accessed: October. 17, 2024. [Online]. Available: https://www.basf.com/no/en/products/plastics-rubber/fairs/BASFatK2016/must_sees/SLENTITE.
GUTEX: _Produkt." Accessed:October. 17, 2024. [Online]. Available: https://gutex-benelux.eu/assortiment/producten/produkt/gutex-thermoflex-1/.